JOURNAL OF MATERIALS SCIENCE **36** (2001) 3221 – 3227

Nanostructured thin palladium-silver membranes: Effects of grain size on gas permeation properties

B. A. McCOOL, Y. S. LIN*
Department of Chemical Engineering, University of Cincinnati, Cincinnati, OH 45221-0171, USA
E-mail: Jlin@alpha.che.uc.edu

Submicron-thick Pd-Ag alloy membranes, prepared on 4 nm pore γ-alumina support by magnetron sputter deposition, are nanocrystalline with a grain (crystallite) size of about 20 nm. The membranes show good selectivity for hydrogen over helium (about 4000 at 300°C). Hydrogen permeation is dominated by the surface reaction steps in 100–200°C with an activation energy of about 30 kJ/mol. Bulk diffusion resistance becomes important at higher temperatures (>200 °C). Grain size is the most critical parameter affecting the hydrogen permeance of the thin nanostructued Pd-Ag membranes. Increase in Pd-Ag grain size from about 20 to 60 nm results in a substantial improvement in hydrogen permeance with a higher apparent activation energy in 100–300°C. Grain growth appears to increase the hydrogen permeability in the bulk phase of the Pd-Ag membranes. Helium permeance through the grain boundary decreases with increasing temperature or hydrogen partial pressure due to grain expansion. Carbonation and the accompanied grain expansion have detrimental effects on the perm-selectivity of the Pd-Ag membranes.

1. Introduction

In the past ten years palladium and palladium silver alloys have gained new attention in the area of hydrogen separation and membrane reactors. Thin films of palladium and alloys of palladium work quite well as hydrogen separation membranes. By supporting these membranes on porous ceramic or metal a thinner membrane layer can be made which in turn reduces the material costs of the membrane. These types of membranes offer much greater mechanical strength, higher permeation flux for H_2, and good permselectivity for H_2 over other gases.

Both chemical and physical methods such as electroless plating [1–5], chemical vapor deposition [6–8] and sputter deposition [9–12] have been successfully used to deposit thin palladium or palladium alloy films on various porous support materials. If synthesized under controlled conditions, the deposited metal films are gas-tight and exhibit good selectivity for hydrogen over other gases. Generally, the electroless plated palladium films are thicker (1–20 μm), with a larger grain size (>0.1 μm) than the sputter-deposited ones. For example, McCool *et al.* [13] reported the sputter deposition synthesis of submicron-thick Pd-Ag films on 4 nm pore γ-alumina supports. The grain size of the Pd-Ag films ranges from about 20 to 50 nm. The CVD palladium membranes have thickness and grain size between those prepared by electroless plating and sputter deposition.

Different thin film preparation methods give thin metal membranes with a different microstructure. It was found that the submicron-thick Pd-Ag membranes prepared by the sputter deposition method have hydrogen permeance lower than the micron-thick Pd-Ag membranes with a larger grain prepared by the electroless plating and CVD methods [8, 10]. Thin Pd-Ag membranes of similar thickness prepared by different methods exhibit a significant difference in hydrogen permeance [8, 14]. Obviously, the microstructure of the Pd-Ag membranes, represented by their grain (crystallite) size, could be an important factor affecting the hydrogen transport in these membranes.

Experimental data showing the effects of the grain size on gas permeation through dense inorganic membranes were seldom reported until very recently. Yeung *et al.* [15] found that hydrogen permeation through electroless plated pure palladium membranes increases with increasing grain size (in the micron to submicron range). Zhang *et al.* [16] reported an increase in oxygen permeation flux through a dense perovskite type ceramic membrane with decreasing grain size (in the micron range). Since the grain size in these studies was determined from scanning electronic micrographs, the grains observed could be aggregates rather than primary cystallites. Essentially no work has been reported on the effects of nano-sized grains on the hydrogen permeation and separation properties of ultrathin Pd-Ag membranes. The main objective of this article is to

* Author to whom all correspondence should be addressed.

present experimental data showing the effects of the microstructure, particularly the grain (crystallite) size, on hydrogen permeation and separation properties of the thin nano-structured Pd-Ag membranes.

2. Experimental

Nano-structured thin Pd-Ag membranes were prepared by dc magnetron sputtering. Each metallic membrane was deposited on the surface of alumina support of about 2 mm thickness and 20 mm diameter. The supports consisted of a 4 nm pore, 5 μm thick γ-alumina layer coated on coarse pore α-alumina disk, and were prepared by the sol-gel method [17]. The membranes were deposited by dc sputtering using a dc/rf magnetron sputtering unit (Plasma Sciences CRC-150) described in details elsewhere [18]. A Pd/Ag (75/25) target was used to deposit the membranes onto the γ-alumina layer of the support. The target to substrate distance was held constant for all runs at a distance of 10 cm. Before each run the sputtering chamber was evacuated to pressures in the range of 10^{-6} Torr and then back filled with ultra high purity argon at a pressure of 5×10^{-3} Torr. For each run the stage (substrate) temperature was held constant at 400°C. The dc power for membrane deposition was varied for each set at 11, 20, 40 and 60 W. Each membrane was deposited over a period of 10–20 min.

The membranes were analyzed by X-ray diffractometer (Siemens, Cu K_α) with a scan from 20 to 50 2θ at a rate of 1° min^{-1} and a step size of 0.1°. The average grain size was estimated by the Scherrer equation [19] from line broadening of Pd/Ag (111) peak (corrected with the equipment peak broadening). Ag concentration in the membranes was calculated from d-spacing value and EDAX analysis. Pd-Ag membrane thickness was measured by SEM coupled with the XRD intensity data [13].

Hydrogen and helium permeances for the disk-shaped membranes were measured in the multigas permeation system described in details in an earlier publication [8]. The system was first heated to 300°C in helium at a rate of 1°C min^{-1} and the gas permeances were measured in decreasing temperature order (300, 250, 200, 150 and 100°C). A feed of 0.25/0.25/0.5 $He/H_2/N_2$ mixture was introduced at a flow rate of 20 ml min^{-1} to the upstream (metallic layer) surface of the membrane disk. Nitrogen was used as the sweep gas in the permeate side. Both feed and permeate sides were at the atmospheric pressure. The composition of the effluents of the sweep was measured by GC and permeance for species hydrogen or helium (species i) calculated by:

$$F_\mathrm{i} = Q_\mathrm{i}/PS(X_\mathrm{i} - Y_\mathrm{i}) \qquad (1)$$

where Q_i, X_i, Y_i are respectively the permeation flow, and upstream and downstream (outlet) molar fractions of species i, P the atmospheric pressure, and S the membrane area. The helium permeance data provide good indicator for the quality of the membranes. The accuracy of the permeation data measured by this method was within 10%.

To study the effects of the grain size on gas permeation, several membranes were heat-treated at high temperature for grain size modification. The grain size modification was carried out in a tubular furnace in helium atmosphere. Three as-synthesized membranes were first characterized by XRD and gas permeation. Then they were heated in helium atmosphere at rate of 1°C min^{-1} to a temperature of 500°C, sintered at 500°C for a period of 6, 10 and 14 hours, respectively, and then cooled back to room temperature at a rate of 1°C min^{-1}. The membranes were then characterized again by XRD and gas permeation following the same procedure described above.

3. Results and discussion

About twenty Pd-Ag membranes with thickness and Ag concentration respectively in the range of 90–600 nm and 8–20% were prepared by sputter deposition in this work. The Pd-Ag thickness and Ag composition were controlled by the DC power and sputtering time [13]. Fig. 1 shows a scanning electronic micrograph of the cross-section of a sputter-deposited membrane. A typical XRD pattern of the as-synthesized alumina supported Pd-Ag membrane prepared in this work is given in Fig. 2. The XRD peak marked with "α" is from the support. All Pd-Ag films prepared in this work exhibited single phase fcc structure. No XRD peaks were found for the top-layer of the support (γ-alumina) as it is X-ray amorphous. The grain (crystallite) sizes of the as synthesized Pd-Ag membranes are in the range of 10–25 nm.

Fig. 3 shows hydrogen and helium permeance of an as-synthesized Pd-Ag membrane. The data for the same membrane after heat-treatment for grain growth are also given in the figure and will be discussed later. As shown this membrane has hydrogen to helium selectivity in the range of 1000–4000 at temperatures higher than 200°C. Most membranes prepared in this work exhibit hydrogen to helium selectivity larger than 100, except for some thinner membranes with lower

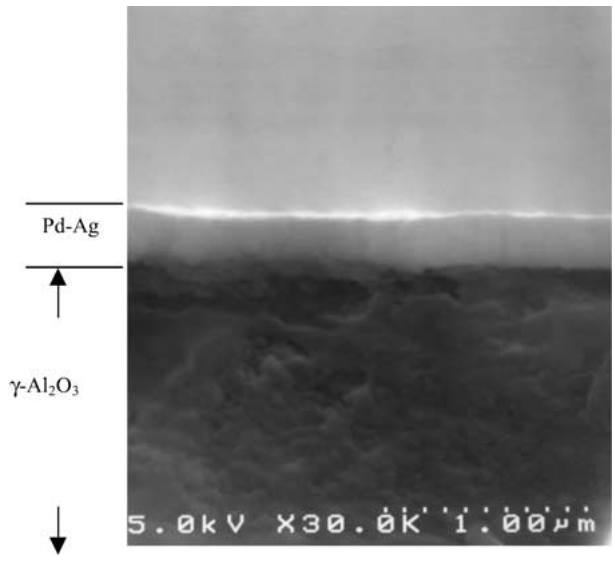

Figure 1 Scanning electronic micrograph showing the cross-section of sputter-deposited Pd-Ag membrane.

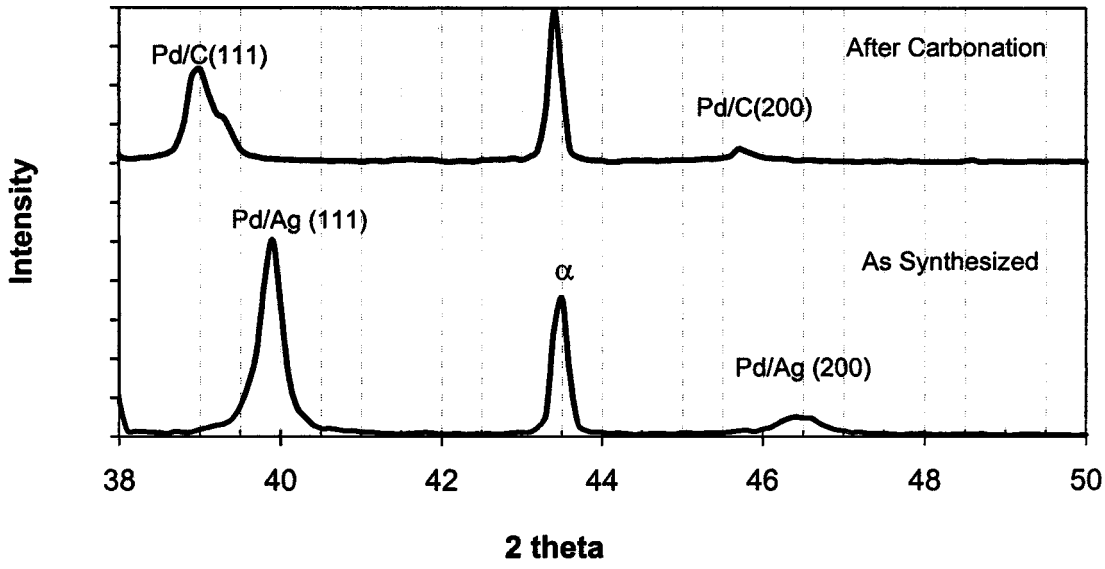

Figure 2 XRD pattern of an as-synthesized Pd-Ag membrane (lower) and that of the same membrane after carbonation poisoning (upper).

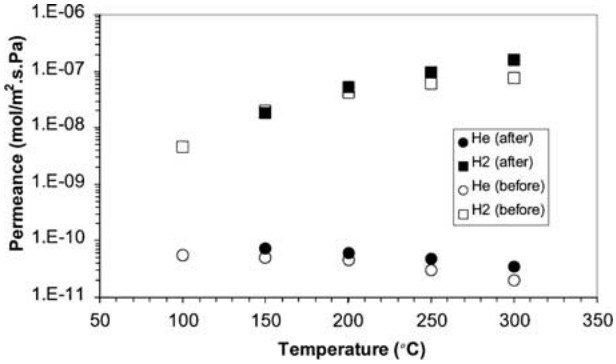

Figure 3 Hydrogen and helium permeance for Pd-Ag membrane (M-6) before and after sintering at 500°C.

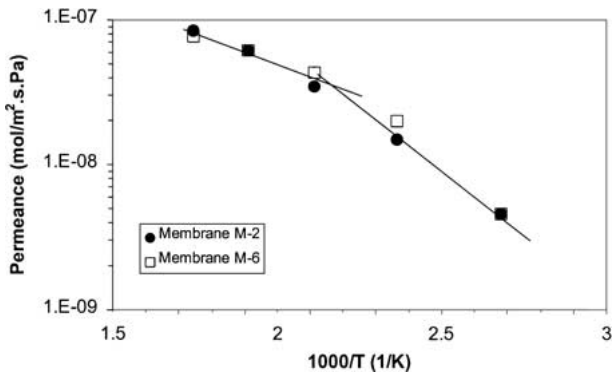

Figure 4 Arrhenius plots of hydrogen permeance for Pd-Ag membranes (M-2 and M-6).

Ag concentrations. The Pd-Ag membranes after these hydrogen permeation experiments had same XRD patterns as the as-synthesized membranes.

Arrhenius plots of hydrogen permeance for two as-synthesized membranes are given in Fig. 4 in the temperature range of 100–300°C. A larger slope is found for permeance data at temperatures lower than 200°C, as shown in Fig. 4. For both membranes the activation energy calculated from the permeance data in the lower temperature range (100–200°C) is respectively about 30 and 33 kJ/mol.

TABLE I Apparent activation energies for hydrogen permeation through ultrathin Pd-Ag membranes of different thickness and composition

Membrane Sample #	Thickness (nm)	Ag%	E (kJ/mol)*
M-2	163	16.1	29.7
M-3	177	18.5	31.3
M-4	325	10.9	29.8
M-6	175	17.6	33.2

*estimated in 100–200°C

The activation energy data listed in Table I for the lower temperature range are much larger than those for thicker membranes (6–10 kJ mol^{-1}) when diffusion of atomic hydrogen in the bulk of the membrane is rate-limiting [9, 14, 20]. In the lower temperature range the surface reaction is more likely to be the rate-limiting step for hydrogen permeation through the ultrathin metal membranes. As temperature increases, the resistance of the surface reaction with a larger activation energy becomes less important as compared to the bulk diffusion resistance. Therefore, the apparent activation energy observed for hydrogen permeation through the ultrathin metal membranes decreases as temperature increases.

The hydrogen permeance flux at 300°C ($P_H = 2$ atm, $P_L = 1$ atm) for a 122 μm thick 25%Ag Pd-Ag membrane prepared by the conventional method is 0.021 $mol/m^2.s$. [20]. Under the same conditions, the flux is 0.2 $mol/m^2.s$ for the 3–5 μm thick CVD Pd membrane [6], 0.1–0.3 mol/m^2 for 4–12 μm thick electroless plated Pd or Pd-Ag membranes [2, 3], and 0.01–0.02 $mol/m^2.s$ for the sputter deposited Pd-Ag membrane with the smallest thickness (0.2–0.5μm). Athayde *et al.* [21] reported hydrogen permeation flux of about 0.002 $mol/m^2.s$ for sputter-deposited 0.05 μm thick Pd-Ag membrane on polymer support at a lower temperature (100°C). This flux is similar to the membranes prepared in this work at this temperature.

It is known that increasing membrane thickness decreases hydrogen permeance (bulk diffusion

TABLE II Characteristics for hydrogen permeation of two Pd-Ag membranes prepared with different DC power (10 min sputtering)

Membrane Sample #	DC Power (W)	Thickness (nm)	Ag%	Grain size (nm)
N-1	11	110	20.4	11
N-2	60	390	13.3	21

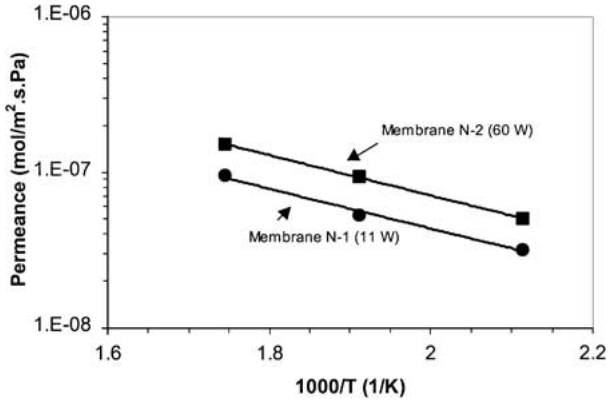

Figure 5 Hydrogen permeance for two Pd-Ag membranes listed in Table II with different grain size, composition and thickness.

rate-limiting) or gives no effects on hydrogen permeance (surface steps rate-limiting) [14], and Pd-Ag membrane with about 23%Ag has the highest hydrogen permeability [22]. No such correlation between the hydrogen permeance and membrane thickness and Ag composition was found in this work for the sputter-deposited thin Pd-Ag membranes. As an example, Table II gives the characteristics of two Pd-Ag membranes with different thickness, Ag concentration and grain size. Fig. 5 shows hydrogen permeance of these two membranes as a function of temperature in 200–300°C. These data correspond to the permeation data given in Fig. 4 in the higher temperature range (where the bulk diffusion dominates hydrogen permeation) and therefore can be correlated by one straight line with a lower activation energy. The thicker membrane with a lower Ag% concentration has a higher hydrogen permeance. For these two membranes, it appears that the grain size is more important in affecting the hydrogen permeation.

Table III lists three Pd-Ag membranes with different thickness, composition and grain size. To show sole effect of the grain size on hydrogen permeation, each membrane was heat-treated at 500°C for grain growth and its hydrogen permeance was measured before and after the heat-treatment. XRD patterns of the Pd-Ag

TABLE III Characteristics of Pd-Ag membranes before and after heat-treatment at 500°C

Membrane Sample #	Thickness (nm)	Ag%	Grain Size (before) (nm)	Heat-Treatment Time (h)	Grain Size (after) (nm)
M-6	175	17.6	13.8	6	41.5
M-9	111	13.0	16.2	10	50.3
M-10	93	13.3	18.0	14	62.0

TABLE IV Hydrogen permeance and selectivity at 300°C for the three Pd-Ag membranes listed in Table III before and after heat-treatment at 500°C

	$J_{H2}(10^{-8}$ mol/m^2.s.Pa)		H_2/He Selectivity	
Membrane #	Before	After	Before	After
M-6	7.69	16.7	3850	4770
M-7	4.56	21.3	36	67
M-10	3.83	18.0	23	45

membranes after the heat-treatment are essentially the same as the as-synthesized membranes (Fig. 2) except that the former have narrower Pd/Ag (100) and (200) peaks than the latter. As shown in Table III, the grain size increased from about 15 nm to 42–62 nm after grain growth modification. Since the heat-treatment would only change the grain (crystallite) size, but not the membrane thickness and composition, a comparison of hydrogen permeance of the same membrane before and after the heat-treatment would indicate the sole effect of the grain size on hydrogen permeation properties.

Hydrogen and helium permeance of membrane M-6 listed in Table III after grain growth modification are compared in Fig. 3 with that before the modification. Hydrogen permeance and hydrogen to helium selectivity at a given temperature for the three membranes before and after the grain growth modification are compared in Table IV. For all the three membranes the grain growth increases hydrogen permeance and selectivity (at 300°C). M-7 and M-10 membranes show much lower selectivity than M-6 membrane due to their smaller membrane thickness making the membranes more prone to the presence of defects during the film formation process. It should be noted that on average the grain growth caused about 2 to 4 fold increase in helium and hydrogen permeance. The increase in helium permeance indicates an enlargement of grain-boundary space or defects through which hydrogen can also permeate by the same mechanism as helium (e.g., Knudsen diffusion), referred to here as the defect flux or permeance. However, the contribution of the defect hydrogen flux to the total hydrogen flux measured is very small. For M-7 membrane at 300°C, for example, the initial hydrogen and helium permeance is respectively about 4.56 and 0.126 (10^{-8}mol/m^2.s.Pa). A 2 fold increase in helium permeance corresponds to an additional defect helium permeance of 0.126 (10^{-8}mol/m^2.s.Pa). Assuming the Knudsen flow in the defects and 4 fold increase in hydrogen permeance after the grain growth, this gives an additional defect hydrogen permeance of 0.178 (10^{-8}mol/m^2.s.Pa), about 1.3% of the hydrogen permeance increase caused by the grain growth modification. Therefore, an increase in hydrogen permeability of the Pd-Ag contributes to the majority of the hydrogen permeance increase caused by the grain growth for the thin Pd-Ag membrane.

The ratio of hydrogen permeance for each Pd/Ag membrane after grain growth modification to that before modification for the three membranes listed in Table III are plotted versus permeation temperature in Fig. 6. As shown, for all three membranes, hydrogen

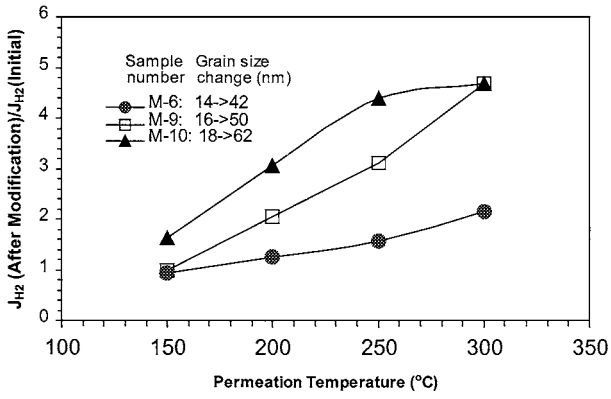

Figure 6 Ratio of hydrogen permeance for three as-synthesized Pd-Ag membranes to that of the same membranes after grain growth modification.

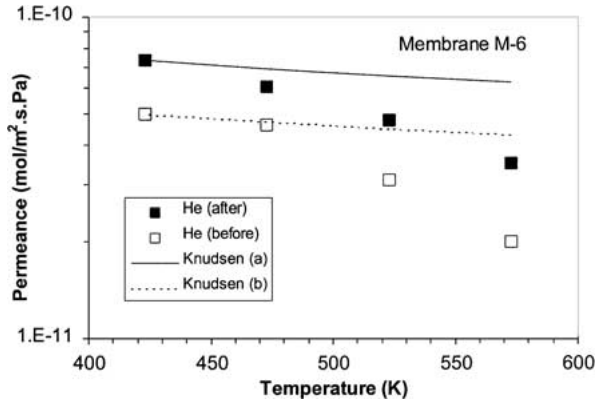

Figure 7 Helium permeation through the Pd-Ag membrane (M-6) before and after grain growth modification as a function of permeation temperature.

permeance after modification is larger than that before modification. Larger grain growth leads to more increase in hydrogen permeance. The membrane with grain size increased from 18 nm to 62 nm exhibits about 5 fold increase in hydrogen permeance at 300°C. Furthermore, grain growth results in more improvement in hydrogen permeance at high temperatures. At 150°C the hydrogen permeance for the membranes shown in Fig. 6 after grain growth is essentially the same as that before the grain growth. Since in the high temperature range the bulk diffusion resistance is more important, the results suggest that the grain growth enhances the hydrogen permeability (product of solubility and diffusion) of the thin metal membranes.

Baxbaum and Maker [2] reported hydrogen permeance of about 1×10^{-6} mol/m^2.s.Pa at 300°C for a 4000 nm thick Pd-Ag membrane prepared by electroless-plating method. The permeance is much larger than the much thinner (200–1000 nm) Pd-Ag membranes prepared by sputter deposition method shown in this work or by the CVD method as reported by Xomeritakis and Lin [18]. The electroless-plated Pd-Ag membranes have a crystallite size of about 600 nm, as estimated from XRD data reported [2], significantly larger than the nanostructured Pd-Ag membranes prepared by the vapor deposition methods. These results suggest that the crystallite size, in addition to the membrane thickness and composition, is an important factor controlling the hydrogen permeation properties of thin Pd-Ag membranes.

The selectivity of a Pd-Ag membrane for hydrogen to helium (or other gases) depends not only on the hydrogen permeability through the dense Pd-Ag grains but also the permeance of helium (or other gases) through the grain boundary or defect pores. Fig. 7 shows helium permeance through a Pd-Ag membrane before and after grain growth modification as a function of permeation temperature. The grain growth results in an increase in helium permeance, indicating a possible rearrangement in the grain boundary structure in the Pd-Ag after the heat-treatment. Such rearrangement increases the grain boundary gap for helium permeation. In both cases, the helium permeance decreases with increasing temperature. Helium permeance at various temperatures using the Knudsen relation ($F_{He} \approx T^{-1/2}$) are also compared in Fig. 7. Increasing temperature results in a more reduction in helium permeance than the effect of temperature on gas permeance based on the Knudsen relation. Grain expansion at higher temperatures narrows the grain boundary gap, reducing helium permeance.

TABLE V Characteristics of other Pd-Ag membranes studied in this work

Membrane Sample #	Thickness (nm)	Ag%
M-5	525	10.4
M-7	522	8.2
M-8	329	11.3

It is known that the lattice parameter of Pd-Ag also increases with increasing concentration of hydrogen dissolved in the Pd-Ag lattice [23, 24]. This suggests that presence of hydrogen would reduce the helium permeance through the grain boundary gap as a result of the grain expansion. Membranes listed in Table V were tested to determine the amount of reduction in helium permeance as a function of feed hydrogen composition. Fig. 8 presents the results of the multiple gas permeation data with membrane M-5. Over a range of 0–20% H_2 feed composition the helium permeance decreases from 1.57×10^{-9} to 7.66×10^{-10} mol m^{-2}s^{-1}Pa^{-1}. In the same composition range, hydrogen permeance remains unchanged. Hydrogen over helium selectivity increases with increasing hydrogen partial pressure.

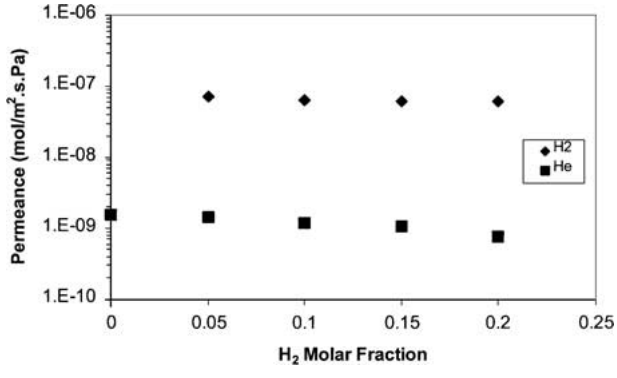

Figure 8 Hydrogen and helium permeance for Pd-Ag membrane (M-5) versus hydrogen concentration in the feed (300°C).

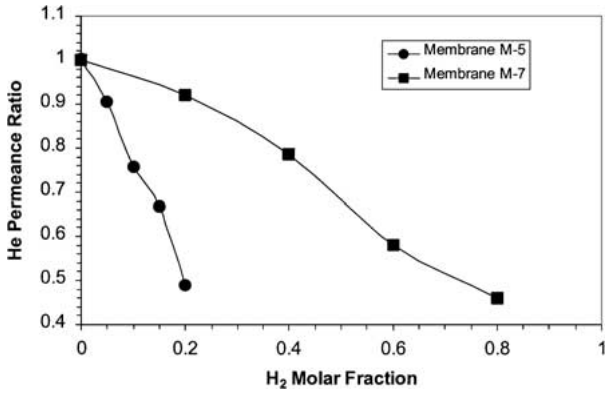

Figure 9 Normalized helium permeance of Pd-Ag membranes as a function of hydrogen molar fraction in the feed (300°C).

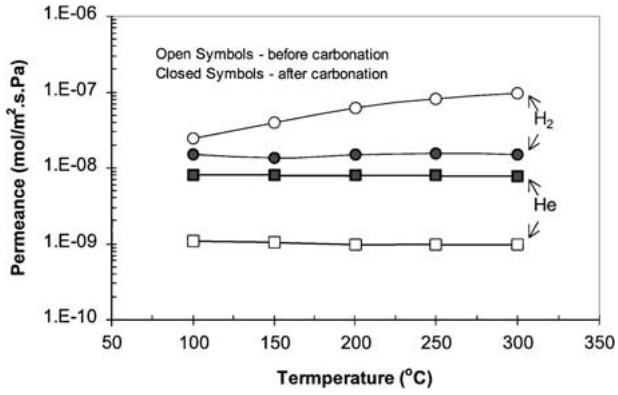

Figure 10 Hydrogen and helium gas permeance of the membrane shown in Fig. 2 before and after carbonation poisoning.

Fig. 9 shows ratio of the helium permeance with presence of hydrogen to that in pure helium for these two membranes tested. For both membranes increasing hydrogen concentration (partial pressure) improves gas-tightness of the Pd-Ag membranes, showing a positive effect of the grain expansion on permselectivity of Pd-Ag membrane in the presence of hydrogen. This effect is more significant for M-5 membrane than M-7 membrane. Hydrogen to helium selectivity for M-5 membrane is over 100 and that for M-7 is about 50. This means that M-5 membrane contains less grain-boundary space or defects than M-7 membrane. Therefore grain expansion due to sorption of hydrogen narrows or reduces the small grain-boundary space or defects more effectively than the large ones.

Increasing hydrogen partial pressure or temperature affects the microstructure of Pd-Ag membranes in a positive manner in terms of perm-selectivity for hydrogen over helium. Grain size increase due to contamination would however have negative effects on separation properties. Some Pd-Ag membranes were contaminated with carbon to test this effect. The membranes were sealed with graphite seals in the permeation cell and heated at 500°C for over one day. Sputter deposited membranes have a mirror like surface, but the surface of the contaminated membranes after this treatment appeared gray and non-reflective. The XRD patterns of such a membrane (sample M-8) after the carbonation is compared in Fig. 2 with that before carbonation. The fcc Pd/Ag (111) and (200) peaks of the Pd-Ag membrane after the treatment are shifted to the left indicating an increase in d-spacing (corresponding to an increase in lattice parameter from 2.87 to 3.24 Angstrom). This shifting was also found in MOCVD Pd membranes due to incomplete conversion of a metal organic precursor [8]. Thus, this heat-treatment resulted in formation of the Pd-Ag-C alloy with an expansion of the lattice (and the grains).

Fig. 10 presents the multiple gas permeation data for the membrane shown in Fig. 2 before and after the carbon contamination heat treatment. The hydrogen permeance is reduced by an order of magnitude after the heat treatment and the helium permeance is increased by nearly an order of magnitude. The H_2/He selectivity is thereby reduced by nearly two orders of magnitude. The incorporation of carbon into the membrane layer has a drastic effect on the performance of the membrane. For the contaminated Pd-Ag membrane, the hydrogen and helium permeation rates are nearly the same. This indicates transport of gases through the defects only and a complete poisoning of the metallic part of the membrane.

4. Conclusions

Submicron-thick nanocrystalline Pd-Ag membranes with high hydrogen to helium selectivity (>1000) can be prepared on porous ceramic supports by the sputter deposition method. Hydrogen permeation through the nanostructured Pd-Ag membranes is controlled by the surface reactions in lower temperatures (<200°C) with activation energy of about 30 kJ/mol. Bulk diffusion resistance becomes important for hydrogen permeation at higher temperature with a lower apparent activation energy. The hydrogen permeation flux through the ultrathin Pd-Ag membranes are similar to thick Pd-Ag membranes with larger grain size prepared by other methods.

Grain (crystallite) size of the thin nanocrystalline Pd-Ag membranes is found to be the key parameter affecting hydrogen permeation properties. Thin Pd-Ag membranes with a larger grain size has a higher hydrogen permeability than the smaller grained Pd-Ag membranes. The grain growth affects primarily the hydrogen permeability in the bulk membrane phase. Grain expansion by increasing temperature or incorporation of hydrogen in Pd-Ag lattice narrows the grain-boundary gap, improving membrane perm-selectivity for hydrogen over other gases. However, Pd-Ag membrane can be carbonized by contacting with graphite resulting in loss of permselectivity for hydrogen over other gases.

The results show that thin nanostructured Pd-Ag membranes do not offer a higher hydrogen permeation as expected. The major advantages of the sputter-deposited Pd-Ag membranes are high productivity and reproducibility of the membrane production and substantial saving of the precious Pd and Ag materials. Higher hydrogen permeance can be achieved by proper annealing the as-synthesized thin Pd-Ag membranes at a high temperature.

Acknowledgement

This work was supported by Petroleum Research Fund administered by the American Chemical Society.

References

1. S. UEMIYA, N. SATO, H. ANDO, Y. KUDE, T. MATSUDA and E. KIKUCHI, *J. Membr. Sci.* **56** (1991) 303.
2. R. E. BUXBAUM and T. L. MARKER, *ibid.* **85** (1993) 29.
3. J. P. COLLINS and J. D. WAY, *Ind. Eng. Chem. Res.* **32** (1993) 3006.
4. K. L. YEUNG and A. VARMA, *AIChE J.* **41** (1995) 2131.
5. N. JEMAA, J. SHU, S. KALIAGUINE and B. P. A. GRANDJEAN, *Ind. Eng. Chem. Res.* **35** (1996) 973.
6. S. YAN, H. MAEDA, K. KUSAKABE and S. MOROOKA, *ibid.* **33** (1994) 616.
7. S. MOROOKA, S. YAN, S. YOKOYAMA and K. KUSKABA, *Sep. Sci. Technol.* **30** (1995) 2887.
8. G. XOMERITAKIS and Y. S. LIN, *AIChE J.* **44** (1998) 174.
9. V. JAYARAMAN, Y. S. LIN, M. PAKALA and R. Y. LIN, *J. Membr. Sci.* **99** (1995) 89.
10. V. JAYARAMAN and Y. S. LIN, *ibid.* **104** (1995) 251.
11. K. J. BRYDEN and J. Y. YING, *Mat. Sci. & Eng.* **A204** (1995) 140.
12. N. M. PEACHY and R. C. DYE *J. Membr. Sci.* **111** (1996) 123.
13. B. A. MCCOOL G. XOMERITAKIS and Y. S. LIN, *ibid.* **167** (1999) 67.
14. T. L. WARD and T. DAO, *ibid.* **153** (1999) 211.
15. K. L YEUNG, S. C. CHRISTIANSEN and A. VARMA, *ibid.* **159** (1999) 107.
16. K. ZHANG, Y. L. YANG, D. PONNUSAMY, A. J. JACOBSON and K. SALAMA, *J. Mater. Sci.* **34** (1999) 2367.
17. C. H. CHANG, R. GOPALAN and Y. S. LIN, *J. Membr. Sci.* **91** (1994) 27.
18. G. XOMERITAKIS and Y. S. LIN, *ibid.* **133** (1997) 217.
19. B. D. CULLITY, "Elements of X-Ray Diffraction," 2nd ed. (Addison-Wesley Publications, Reading, Mass., 1978).
20. F. J. ACKERMAN and G. J. KOSKINAS, *J. Chem. Eng. Data* **7** (1972) 51.
21. A. L. ATHAYDE, R. W. BAKER and P. NGUYEN, *J. Membr. Sci.* **94** (1994) 299.
22. F. A. LEWIS, "The Palladium Hydrogen System" (Academic Press, New York, 1967).
23. J. A. EASTMAN, L. J. THOMPSON and B. J. KESTEL, *Phys. Rev. B* **48** (1993) 84.
24. B. L. BLACKFORD and C. S. ARNOLD, *J. Appl. Phys.* **76** (1994) 4054.

Received 1 June
and accepted 24 October 2000